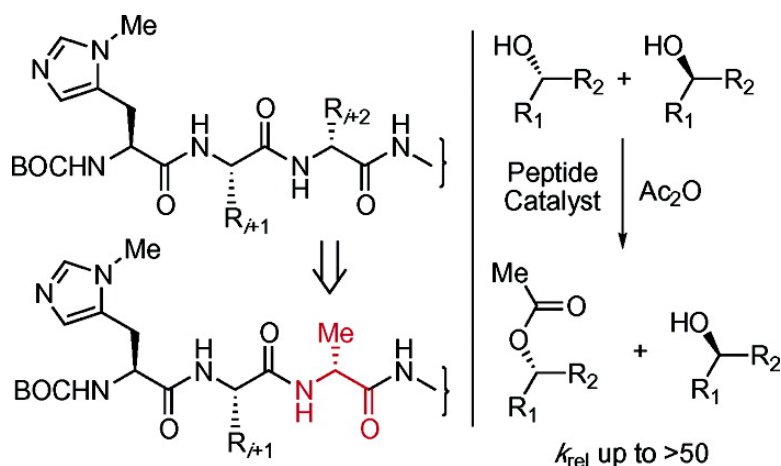


## Structure-Selectivity Relationships and Structure for a Peptide-Based Enantioselective Acylation Catalyst

Matthew B. Fierman, Daniel J. O'Leary, Wayne E. Steinmetz, and Scott J. Miller

*J. Am. Chem. Soc.*, **2004**, 126 (22), 6967-6971 • DOI: 10.1021/ja049661c • Publication Date (Web): 15 May 2004

Downloaded from <http://pubs.acs.org> on March 31, 2009



### More About This Article

Additional resources and features associated with this article are available within the HTML version:

- Supporting Information
- Links to the 8 articles that cite this article, as of the time of this article download
- Access to high resolution figures
- Links to articles and content related to this article
- Copyright permission to reproduce figures and/or text from this article

[View the Full Text HTML](#)

## Structure-Selectivity Relationships and Structure for a Peptide-Based Enantioselective Acylation Catalyst

Matthew B. Fierman,<sup>†</sup> Daniel J. O'Leary,<sup>‡</sup> Wayne E. Steinmetz,<sup>‡</sup> and Scott J. Miller<sup>\*†</sup>

Contribution from the Department of Chemistry, Merkert Chemistry Center, Boston College, Chestnut Hill, Massachusetts 02467-3860 and Department of Chemistry, Pomona College, 645 North College Avenue, Claremont, California 91711

Received January 19, 2004; E-mail: scott.miller.1@bc.edu

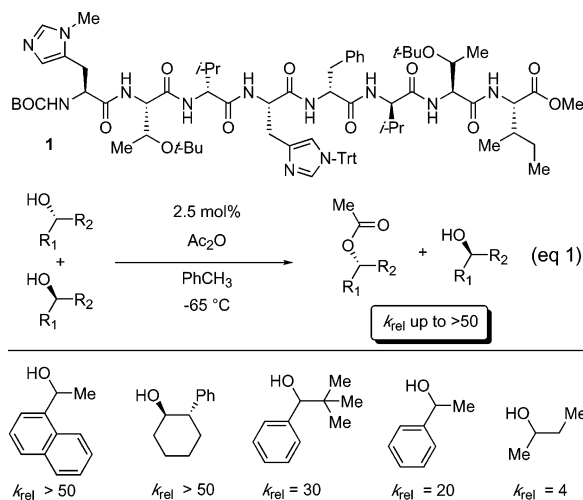
**Abstract:** Studies of analogues of a recently discovered enantioselective peptide-based catalyst for enantioselective acylation reactions have led to mechanistic insight and improved catalysts. Systematic replacement of each residue within the parent peptide with alanine of the appropriate stereochemistry allows for an unambiguous evaluation of the kinetic role of each amino acid side chain in the catalyst. The results of the alanine scan support a bifunctional catalysis mechanism at the heart of the origin of enantioselectivity. In addition, an experimentally derived solution structure of the peptide-based catalyst is presented that supports a key role for each residue within the peptide chain.

### Introduction

The search for low molecular weight asymmetric catalysts has spawned the development of many interesting compounds that function as enantioselective catalysts.<sup>1</sup> Amino acid and peptide-based catalysts offer intriguing analogies to enzymatic systems.<sup>2</sup> Their reliance on similar conformational determinants and functional group arrays are reminiscent of those present in protein-based catalysts. In this context, we report an experimental study of an effective peptide-based catalyst that points to a bifunctional mechanism of action.

We recently reported that octapeptide **1** functions as an effective asymmetric acylation catalyst for the kinetic resolution of a variety of racemic secondary alcohol substrates (eq 1).<sup>3–5</sup> Notably, the catalyst exhibits remarkable activity: it effects kinetic resolution of its substrates at the 2.5 mol % level (or lower), with conversions between 40 and 50% at  $-65\text{ }^{\circ}\text{C}$ ,

generally within 12–24 h. Many substrates also provide similar results with a catalyst loading of 0.5 mol %, provided a tertiary amine base (*i*-Pr<sub>2</sub>NEt) is employed as an additive. The degree of enantioselection that catalyst **1** provides is also of note. For example, some substrates examined afforded  $k_{\text{rel}}$  values of  $>50$  (e.g.,  $\alpha$ -naphthylethanol) whereas even *sec*-butanol exhibits  $k_{\text{rel}} = 4$ .<sup>6</sup> Because peptide **1** was discovered through the application of combinatorial techniques,<sup>7</sup> its mechanism of action was unknown at the time of discovery. Nevertheless, we report herein progress in establishing the key features that contribute mechanistically to the catalyst's activity and enantioselectivity. At the same time, these studies have led to improved catalysts for at least one substrate.

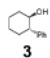
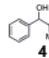


<sup>†</sup> Department of Chemistry, Merkert Chemistry Center, Boston College.

<sup>‡</sup> Department of Chemistry, Pomona College.

- (1) *Comprehensive Asymmetric Catalysis*; Jacobsen, E. N., Pfaltz, A., Yamamoto, H., Eds.; Springer-Verlag: Berlin Heidelberg, 1999; Vols. I–III.
- (2) (a) Dalko, P. I.; Moisan, L. *Angew. Chem., Int. Ed.* **2001**, *40*, 3726–3748. (b) List, B. *Synlett* **2001**, *11*, 1675–1686. (c) List, B. *Tetrahedron* **2002**, *58*, 5573–5590. (d) Jarvo, E. R.; Miller, S. J. *Tetrahedron* **2002**, *58*, 2481–2495. (e) Movassaghi, M.; Jacobsen, E. N. *Science* **2002**, *298*, 1904–1905.
- (3) Copeland, G. T.; Miller, S. J. *J. Am. Chem. Soc.* **2001**, *123*, 6496–6502.
- (4) For reviews, see: (a) Spivey, A. C.; Maddaford, A.; Redgrave, A. J. *Org. Prep. Proc. Int.* **2000**, *32*, 331–365. (b) Jarvo, E. R.; Miller, S. J. "Asymmetric Acylation" In *Comprehensive Asymmetric Catalysis, Supplement 1*; Jacobsen, E. N., Pfaltz, A., Yamamoto, H., Eds.; Springer-Verlag: Berlin Heidelberg, 2004; Chapter 43.
- (5) For other representative nonenzymatic catalysts that effect kinetic resolution of racemic alcohols by acylation, see: (a) Fu, G. C. *Acc. Chem. Res.* **2000**, *33*, 412–420. (b) Vedejs, E.; Daugulis, O. *J. Am. Chem. Soc.* **1999**, *121*, 5813–5814. (c) Spivey, A. C.; Fekner, T.; Spey, S. E. *J. Org. Chem.* **2000**, *65*, 3154–3159. (d) Sano, T.; Miyata, H.; Oriyama, T. *Enantiomer* **2000**, *5*, 119–123. (e) Kawabata, T.; Nagato, M.; Takasu, K.; Fuji, K. *J. Am. Chem. Soc.* **1997**, *119*, 3169–3170.

**Table 1.** Alanine Scan Data for Peptides (0.5 Mol %) in Kinetic Resolutions<sup>a</sup>

Catalyst	Substrate:		
<b>1</b>		$k_{rel} > 50$ (Conv = 45%)	$k_{rel} = 17$ (Conv = 25%)
<b>2a</b>	Ala Position: (i+7)	$k_{rel} > 50$ (Conv = 45%)	$k_{rel} = 14$ (Conv = 27%)
<b>2b</b>	(i+6)	$k_{rel} = 50$ (Conv = 46%)	$k_{rel} = 10$ (Conv = 17%)
<b>2c</b>	(i+5)	$k_{rel} = 48$ (Conv = 47%)	$k_{rel} = 15$ (Conv = 26%)
<b>2d</b>	(i+4)	$k_{rel} > 50$ (Conv = 54%)	$k_{rel} = 18$ (Conv = 26%)
<b>2e</b>	(i+3)	Conv < 5%	Conv < 5%
<b>2f</b>	(i+2)	$k_{rel} > 50$ (Conv = 37%)	$k_{rel} > 50$ (Conv = 35%)
<b>2g</b>	(i+1)	$k_{rel} > 50$ (Conv = 47%)	$k_{rel} = 47$ (Conv = 36%)
<b>2h</b>	(i)	Conv < 5%	Conv < 5%

<sup>a</sup> Kinetic resolutions were performed with 0.5 mol% catalyst in the presence of 0.4 equiv of Hunig's base (PhCH<sub>3</sub> solvent, -65 °C). Reactions were uniformly quenched after 12 h by addition of MeOH, followed by warming the reaction mixture to room temperature. Reported data represent the average of 2–3 runs.

## Results and Discussion

**Analogue Catalysts.** The “Alanine Scan” represents a powerful tool in peptide and protein chemistry for the elucidation of the roles of key residues in contributing to the overall function of a given sequence.<sup>8</sup> In this approach, individual residues are systematically replaced with alanine to produce a new set of peptides wherein the role of the residue undergoing substitution is probed. We prepared a set of alanine scan peptides **2a–2h** and examined them in kinetic resolutions with the goal of gaining insight into the role of each residue within catalyst **1**. The specific structures of each peptide are shown in Table 1. In each case, the stereochemical configuration of the alanine that was inserted was preserved with respect to the overall configuration of the parent peptide **1**.

The eight new catalysts were then screened against two representative racemic substrates, *trans*-2-phenyl-cyclohexanol (**3**) and 1-phenyl-2,2-dimethyl-propanol (**4**), with revealing results. Cyclohexanol **3** is an excellent substrate for peptide **1**, affording a  $k_{rel} > 50$  when catalyst **1** is employed under optimized conditions. Notably, peptides **2a**, **2b**, **2c**, and **2d**, wherein the residues at the *i*+4 through the *i*+7 positions have been replaced with alanine, are all effective enantioselective

catalysts, each performing the kinetic resolution of substrate **3** with  $k_{rel} > 48$ . On the other hand, peptide **2e**, where the central (*i*+3) His residue is replaced with alanine, is a poor catalyst both in terms of enantioselectivity and rate; with this peptide, the reaction essentially does not proceed under the conditions of the experiment. Peptides **2f** and **2g**, with the *i*+2 and the *i*+1 positions replaced with alanine, once again resemble the parent catalyst **1** in terms of selectivity ( $k_{rel} > 50$ ). But, peptide **2h**, with the *N*-terminal residue replaced with alanine, is not a catalyst for the reaction under the prescribed conditions.

These results clearly highlight the importance of the two His residues in combining to make for a functional (active and selective) peptide catalyst. Given that one of the imidazoles is sterically unencumbered (that of the *N*-terminal  $\pi$ -methyl histidine), and one is sterically encumbered (that of the *i*+3  $\tau$ -trityl histidine), it is tempting to suggest that the former is playing the role of a nucleophilic catalyst, while the latter is serving as a base.<sup>9</sup> While this possibility remains to be established, it is nonetheless clear from the data that peptide **1** is likely a bifunctional catalyst, with two specific side chains critical for activity.

Less clear from the initial data is the role of the nonhistidyl residues in contributing to enantioselectivity. To attempt to glean information on this point, we applied the alanine scan peptides to a substrate that was less effective under catalysis by peptide **1**. Racemic alcohol **4** presents an interesting case study in this regard since it reacts slowly in acylation reactions with an observed  $k_{rel} = 17$  with peptide **1** under low catalyst loading conditions (0.5 mol %).<sup>10</sup> Thus, substrate **4** affords the possibility of observing more subtle effects, including catalyst improvements; substrate **3** provides a more limited opportunity to observe primarily erosion in catalyst performance.

With substrate **4**, the alanine scan provided qualitatively similar data in comparison to that obtained with substrate **3**. However, we observed a dramatic quantitative improvement in the efficiency of the kinetic resolution with two of the peptides. With substrate **4**, peptides **2a**, **2b**, **2c**, and **2d** afford rate and selectivity data that are moderately lower ( $k_{rel} = 10–18$ , conv = 17–27%) than with original peptide **1**. Peptides **2e** and **2h** are, as with substrate **3**, ineffective under the reaction conditions. However, peptides **2f** and **2g** are *significantly improved* with respect to reaction selectivity in comparison to both original peptide **1**, and the other alanine scan peptides. Peptide **2f** affords  $k_{rel} > 50$  (35% conversion), while peptide **2g** exhibits  $k_{rel} = 47$  (36% conversion).

It is plausible that the insertion of alanine into either the *i*+1 or *i*+2 position of peptide **1** (in place of the sterically demanding *tert*-butyl-threonine and D-valine residues, respectively) provides a relief of steric congestion in the stereodifferentiating transition states for the very bulky alcohol **4**. Given the possibility that the two imidazoles might be working together through a

(6) S-values (=  $k_{rel}$ ) were calculated according to the method of Kagan. See: (a) Kagan, H. B.; Fiaud, J. C. *Top. Stereochem.* **1988**, *18*, 249–330. (b) Reaction selectivities and conversions were determined with the methods we reported previously (ref 3).

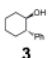
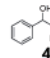
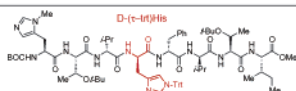
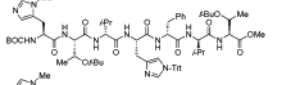
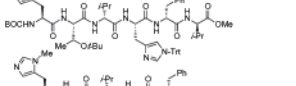
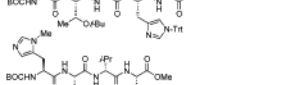
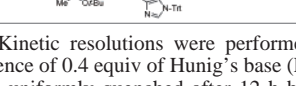
(7) Copeland, G. T.; Miller, S. J. *J. Am. Chem. Soc.* **1999**, *121*, 4306–4307.

(8) Morrison, K. L.; Weiss, G. A. *Curr. Opin. Chem. Biol.* **2001**, *5*, 302–307, and references therein.

(9) Nucleophilic versus general base catalysis with alkylimidazoles has been a subject of some debate. We have adopted the nucleophilic paradigm for the sterically unencumbered moiety for this analysis. (a) Guibe-Jampel, E.; Bram, G.; Vilkas, M. *Bull. Soc. Chim. Fr.* **1973**, 1021–1027. (b) Höfle, G.; Steglich, W.; Vorbrüggen, H. *Angew. Chem., Int. Ed. Engl.* **1978**, *17*, 569–583. (c) Pandit, N. K.; Connors, K. A. *J. Pharm. Sci.* **1982**, *71*, 485–491.

(10) Substrate **4** undergoes kinetic resolution with  $k_{rel} = 30$  when 2.5 mol % peptide **1** is employed as the catalyst. For this substrate, extended reaction times (48–72 h) are required to achieve 40–50% conversion.

**Table 2.** Data for Analogue Peptides (0.5 Mol %) in Kinetic Resolutions<sup>a</sup>

Catalyst	Substrate: 	
<b>5</b> 	$k_{\text{rel}} = 1.4$ (Conv = 22%)	$k_{\text{rel}} = 2.6$ (Conv < 10%)
<b>6</b> 	$k_{\text{rel}} = 11$ (Conv = 52%)	$k_{\text{rel}} = 2.2$ (Conv = 22%)
<b>7</b> 	$k_{\text{rel}} = 2.4$ (Conv = 57%)	$k_{\text{rel}} = 4.2$ (Conv = 29%)
<b>8</b> 	$k_{\text{rel}} = 1.7$ (Conv = 18%)	$k_{\text{rel}} < 2$ (Conv < 10%)
<b>9</b> 	$k_{\text{rel}} = 1.8$ (Conv = 14%)	$k_{\text{rel}} < 2$ (Conv < 10%)

<sup>a</sup> Kinetic resolutions were performed with 0.5 mol% catalyst in the presence of 0.4 equiv of Hunig's base (PhCH<sub>3</sub> solvent, -65 °C). Reactions were uniformly quenched after 12 h by addition of MeOH, followed by warming the reaction mixture to room temperature.

bifunctional catalysis mechanism, the sterics of the intervening residues could indeed be involved in catalyst-substrate contacts.

In addition to the alanine scan peptides, we have prepared several others in an attempt to understand the SAR of peptide **1** in asymmetric acylations. For example, the stereochemical identity of the residues likely plays a significant role in defining the key secondary structure of the active catalyst. Peptide **5** (Table 2), containing a  $\tau$ -trityl-D-histidine at the  $i+3$  position (in place of the L-residue of the parent **1**) leads to a peptide that affords dramatically reduced activity and selectivity in the attempted resolution of alcohols **3** ( $k_{\text{rel}} = 1.4$ , conversion 22%) and **4** ( $k_{\text{rel}} = 2.6$ , conversion < 10%).

We also examined truncated versions of peptide **1** in an attempt to probe the role of the residues remote from the functional *N*-terminal histidine residue (Table 2, **6-9**). For example, in kinetic resolutions of substrates **3** and **4**, heptamer **6** provides greatly reduced selectivities (substrate **3**:  $k_{\text{rel}} = 11$ , conversion = 52%; substrate **4**:  $k_{\text{rel}} = 2.2$ , conversion = 22%). Hexamer **7** affords further reductions in selectivity (substrate **3**:  $k_{\text{rel}} = 2.4$ , conversion = 57%; substrate **4**:  $k_{\text{rel}} = 4.2$ , conversion = 29%). Both pentamer **8** and tetramer **9** exhibit dramatically reduced activity and selectivity relative to the parent octamer in attempted kinetic resolutions (substrate **3** and **4**, catalysts **8** or **9**:  $k_{\text{rel}} < 2$ , conversion < 20%). These data point to a key role for residues  $i+4$  through  $i+7$  in stabilizing a robust three-dimensional structure that promotes optimal activity and selectivity.

**Solution-Phase NMR Structure of Peptide 1.** Since peptide **1** was derived from a combinatorial screening study, not only were the basic mechanistic features of its action unclear at the point of discovery, so too were its basic structural features. We therefore performed a multidimensional NMR study to determine the basic features of the three-dimensional conformation of the catalyst.

**Experimental Aspects.** Several caveats about the NMR experiments are of note. First, all NMR data were recorded with peptide **1** dissolved in CDCl<sub>3</sub>, rather than the toluene solution of the kinetic resolutions. This decision reflects superior

dispersion of the peptide proton resonances in this deuterated solvent. While it is certainly possible that peptide conformation may be different in the two solvents, we opted for CDCl<sub>3</sub> rationalizing that our data would be superior, and that these two nonpolar solvents might be sufficiently similar to allow for the possibility of analogous structures (i.e., the comparison would be more reasonable than that between, for example CD<sub>3</sub>-OD and toluene-*D*<sub>8</sub>.) Second, we elected to make NMR measurements at room temperature, rather than at the -65 °C of the kinetic resolutions. While reaction selectivities do erode at higher temperatures, and in chlorinated solvent, we opted for these conditions to facilitate NMR analysis. We recognize that these two alterations could lead to a structural derivation somewhat outside the conditions of the experimental kinetic resolutions.<sup>11</sup> Nevertheless, since the basic secondary structure exhibited by peptide sequences such as **1** was unknown at the outset, we felt that even a structure exhibited under these conditions could be a useful guide for mechanistic analysis, and perhaps future catalyst design. In addition, under these conditions, the NMR spectra were sharp and well resolved.

NMR samples were prepared by dissolving peptide **1** in CDCl<sub>3</sub> ( $c = 7$  mM). Samples were degassed and sealed under nitrogen. 1D <sup>1</sup>H, 2D gs-COSY,<sup>12</sup> TOCSY,<sup>13</sup> and T-ROESY <sup>1</sup>H<sup>14</sup> spectra were obtained on a Bruker Avance DPX 400 MHz NMR spectrometer. These data were used for chemical shift assignment and provided a useful set of ROE contacts. In particular, acquisition parameters for 2D T-ROESY experiments were 1.05 Hz/pt digital resolution, 512 FIDs recorded, each consisting of 64 scans and 4096 data points, 600 ms spin lock consisting of 4054 cycles of phase-shifted pairs of 74  $\mu$ s 180° pulses, and 1.9 s relaxation delay. 1D GOESYTR<sup>14</sup> experiments were conducted at 500 MHz on a Varian Unity-Inova spectrometer for the purpose of clarifying weak through-space interactions observed in the 400 MHz data set. 1D GOESYTR spectra were acquired with 600 ms spin lock, 1024 scans and 8 K data pts.<sup>15</sup>

Conservative interproton distance restraints were obtained from the 2D ROESY spectrum using a method related to that developed by Wüthrich.<sup>16</sup> Pairs of protons separated by three bonds were treated as sequential. If the calculated distance was 3.0 Å or less, then an upper bound of 3.0 Å was applied. Pairs of protons separated by more than three bonds, or which reside on separate residues were treated conservatively and assigned an upper bound of 4.0 Å regardless of calculated distance. For ROE restraints involving unresolvable methylene or methyl protons, the restraint was applied from the carbon of the unresolvable proton to the proton with which it is coupled; a correction of 1.0 Å was applied to that restraint.

To thoroughly search the conformational space available to peptide **1**, we used 22,000 iterations of a random search algorithm employing the MMFF94s force field for energy evaluation.<sup>17</sup> Initial searches employed the unambiguously

(11) A direct comparison of the catalytic performance of the peptide in chloroform is difficult due to the freezing of this reaction mixture at -65 °C.

(12) Hurd, R. E. *J. Magn. Reson.* **1990**, *87*, 422–428.

(13) Bax, A.; Davis, D. G. *J. Magn. Reson.* **1985**, *65*, 355–360.

(14) Hwang, T.-L.; Shaka A. J. *J. Am. Chem. Soc.* **1992**, *114*, 3157–3159.

(15) See Supporting Information for details.

(16) (a) Wüthrich, K. *NMR of Proteins and Nucleic Acids*; Wiley-Interscience: New York, 1986. (b) Steinmetz, W. E.; Sadowsky, J. D.; Rice, J. S.; Roberts, J. J.; Bui, Y. K. *Magn. Reson. Chem.* **2001**, *39*, 163–172.

(17) (a) Available in Sybyl 6.9 (Tripos Software, St. Louis, MO.) (b) Halgren, T. J. *Comput. Chem.* **1999**, *20*, 720–729.

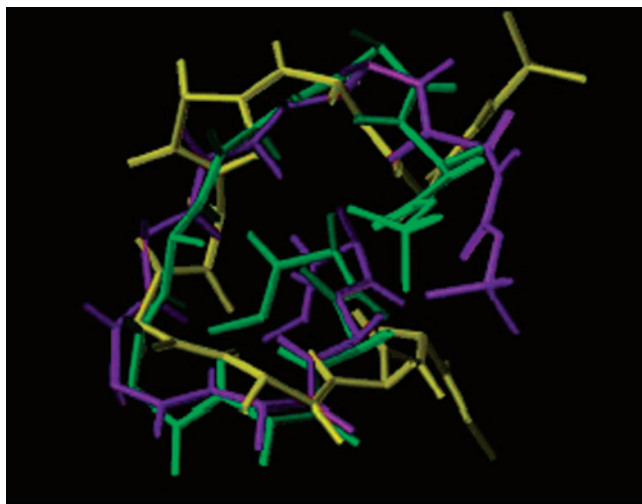


**Figure 1.** Overlay of low energy conformers representative of each structural types. (Type A shown in Green; Type B in purple; Type C in Yello).

assigned rOe restraints from ROESY spectra. All generated conformers with an energy 5 kcal/mol higher than the lowest energy conformer were immediately discarded. Of the remaining low energy conformers, only the ones which allowed assignment of previously ambiguous ROE data and suggested a previously undetected cross-peak confirmed by a GOESYTR experiment were retained. These new rOe restraints were added for final rounds of calculation (100,000 iterations). The final solution phase structures were generated using a total of 25 distance restraints. Nineteen final structures were generated within 5 kcal/mol of the lowest energy conformer.

**Analysis.** Each of the nineteen final conformers fit into three structural families. A representative structure from each is overlaid in Figure 1 (average backbone-RMSD across representative members:  $1.5 \pm 0.81$  Å). Of the three, two are very similar (**A** in green; **B** in purple, each differing by only a small extent along the backbone). Whereas conformer **A** was found once, conformer **B** was found seventeen times. The third family (**C**, in yellow) is quite distinct. Family **C**, populated only once by the lowest energy conformer, is similar to **A** and **B** near the

C-terminal region of the sequence ( $i+4$  through  $i+7$ ); however, significant variation exists in the vicinity of the L-trityl-histidine residue, introducing a kink in the backbone that continues with the N-terminus coiling in the opposite direction in comparison to the other two families. Residues  $i+4$  through  $i+7$  form a tight turn which is especially well defined in the **C** structure. All of the final conformers have minimized energies in the 281–286 kcal/mol range, with no violations of distance constraints greater than 0.11 Å. These minor violations contribute at most 1.1 kcal/mol to the penalty function. The narrow range of energies indicates that all three structures may have comparable populations. This inference is supported by the values of the  $^3J_{\text{NH},\alpha\text{H}}$  and  $^3J_{\alpha\text{H},\beta\text{H}}$  coupling constants (Supporting Information) which provide information on the  $\phi$  and  $\chi$  dihedral angles via the Karplus equation. The total set of coupling constants cannot be reconciled with the predominance of a single structural type but is consistent with conformational averaging over all three types.

It is important to note that in all of the structural families the two histidine side chains are remote from one another. Figure 2 depicts **A**, **B**, and **C** with the imidazole side chains highlighted in orange. Given that the alanine scan and SAR studies indicate that both histidine residues are required for catalyst selectivity and activity, there remains considerable room for speculation on the nature of bifunctional catalysis. For example, if one proposes that the  $\pi$ -methyl-histidine (residue  $i$ ) functions as a catalytic nucleophile, and the  $\tau$ -trityl-histidine (residue  $i+3$ ) as a general base, then a conformational change for the peptide might result upon entrance of **1** into the catalytic cycle (i.e., upon formation of the acyl imidazolium intermediate). Of note, in all three conformer types, the  $\pi$ -methyl-histidine imidazole is solvent exposed, consistent with the possibility of catalyst activation as the first step of the catalytic cycle. Reorganization of chiral space upon nucleophile activation could also be driven by imidazolium ion stabilization.<sup>18</sup>

Alternative interpretations involving a nonobvious role for the internal ( $i+3$ )  $\tau$ -trityl-histidine residue also exist. For example, implicit in each of the low energy structures is a ground-state hydrogen bond between the imidazole  $\pi$ -nitrogen

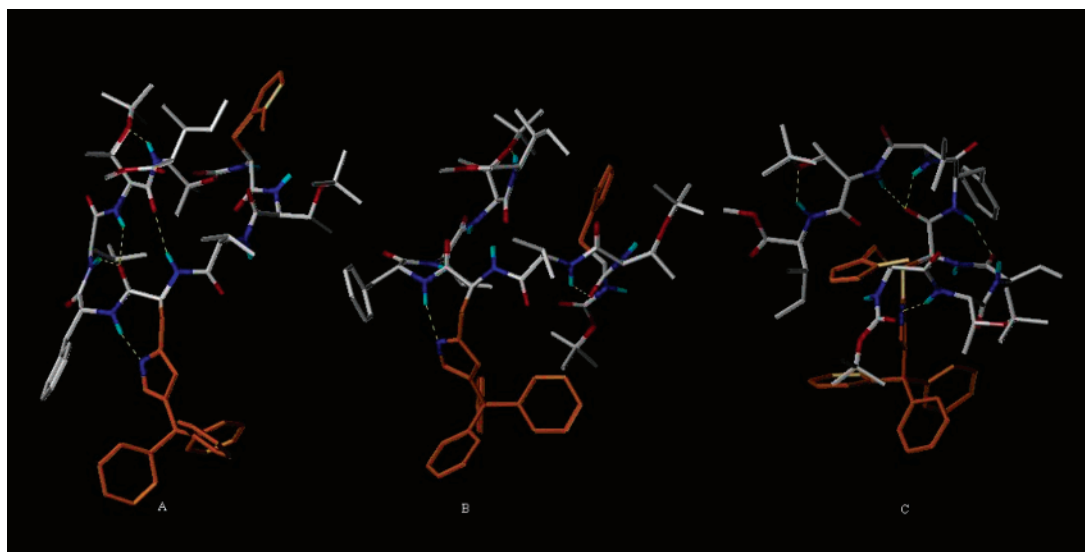


**Figure 2.** Representative members of each family of structures. Imidazole sidechains colored orange and computationally derived hydrogen bonds drawn in yellow hash lines.

and a backbone NH. While this interaction may contribute to secondary structural stabilization, it may also serve to transmit heightened basicity to the corresponding backbone carbonyl oxygen. This carbonyl, in each case disposed to the *N*-terminal side of the catalyst (more proximal to the  $\pi$ -methyl-histidine residue) could then serve as a general base (or a transient, secondary nucleophile) within the bifunctional catalyst. Such cooperative catalytic diads and triads are well-known in enzymatic catalysis. Their definitive documentation in synthetic organocatalysts must await further study. Nevertheless, the ground-state hydrogen bonding between a putative catalytic histidine side chain to a peptide backbone is preceded in low molecular weight catalytic peptides that mediate enantioselective azidation.<sup>19</sup>

## Conclusion

In conclusion, application of the alanine scan technique to a class of peptide-based enantioselective acylation catalysts has increased our understanding of the mode of catalyst action. Octapeptide **1** depends critically on each residue and the presence of two His residues to obtain a highly active and selective profile for the reported acylations. In addition, the alanine scan approach has identified two peptides that are improved catalysts for a typically difficult substrate. A derived solution NMR structure has suggested three related three-dimensional conformations for the catalytic peptide. The ground

state structure, in combination with the alanine scan data, suggest that a bifunctional catalysis mechanism may be consistent with a conformational change during the reaction coordinate, or more subtle cooperative effects among components of the catalyst structure. The application of these and other techniques to mechanistic study and optimization may contribute to next-generation catalysts in this family that harbor both additional improvements and new insights into their mechanisms.

**Acknowledgment.** This research is supported by the U.S. National Science Foundation (CHE-0236591). We are also grateful to Merck Research Laboratories and Pfizer Global Research for research support. S.J.M. is a Fellow of the Alfred P. Sloan Foundation and a Camille Dreyfus Teacher–Scholar. D.J.O. is a Henry Dreyfus Teacher–Scholar.

**Supporting Information Available:** Experimental procedures and product characterization for all new compounds synthesized. For the structure determination of octapeptide **1**: complete proton chemical shift assignments, interproton distance restraints, and representative 1D- and 2D-NMR spectra. This material is free of charge via the Internet at <http://pubs.acs.org>.

JA049661C

(18) See ref 5e.

(19) (a) Guerin, D. J.; Miller, S. J. *J. Am. Chem. Soc.* **2002**, *124*, 2134–2136.  
(b) Blank, J. T.; Guerin, D. J.; Miller, S. J. *Org. Lett.* **2000**, *2*, 1247–1249.